

Monopole and vortex condensation in lattice pure gauge theories

Paolo Cea^{1,2,*} and Leonardo Cosmai^{2,†}

¹*Dipartimento Interateneo di Fisica, Università di Bari, I-70126 Bari, Italy*

²*INFN - Sezione di Bari, I-70126 Bari, Italy*

March, 2001

Abstract

We study monopole and vortex condensation in lattice pure gauge theories. To detect condensation we use a disorder parameter defined in terms of a gauge-invariant effective action built-up using the lattice Schrödinger functional. In the confined phase of U(1) gauge theory monopoles condense at variance with vortices that do not show condensation. For SU(2) and SU(3) lattice gauge theories we observe condensation of Abelian monopoles and vortices in the confined phase. In the case of SU(3) we study various types of Abelian vortices and monopoles defined in terms of the λ_3 and λ_8 diagonal generators and their linear combinations.

PACS number(s): 11.15.Ha

*Electronic address: Paolo.Cea@bari.infn.it

†Electronic address: Leonardo.Cosmai@bari.infn.it

I. INTRODUCTION

The color confinement as dual superconductivity of the vacuum in gauge theories has been proposed since long time ago by G. 't Hooft [1] and S. Mandelstam [2]. In this scenario the confining vacuum behaves like a magnetic (dual) superconductor. The dual superconductivity hypothesis relies upon the very general assumption that the dual superconductivity of the ground state is realized if there is condensation of Abelian magnetic monopoles. Indeed, recent lattice calculations have given evidence of the condensation of Abelian magnetic monopoles [3–8]. On the other hand, recently, numerical evidence has emerged in favor of the so called center vortex picture [9–22], where the vacuum consists of a coherent condensate of magnetic flux tubes. Also this theoretical proposal has been advanced long time ago [23–29].

In this paper we compare the dual superconductivity scenario with the vortex condensate picture both in Abelian and non Abelian pure gauge lattice theories. A partial account of the results discussed in the present paper has been reported in Ref. [30]. In this work we do not consider the center vortices. Instead we study the Abelian vortices which eventually give rise to a coherent condensate of Abelian magnetic flux tubes.

To detect condensation we employ a disorder parameter defined at zero temperature in terms of a gauge-invariant lattice Schrödinger functional [31–33], and at finite temperature in terms of a thermal partition functional [7, 8].

To investigate the dynamics of the vacuum at zero temperature we introduced [31–33] a gauge-invariant effective action for external static (i.e. time-independent) background field defined by means of the lattice Schrödinger functional

$$\mathcal{Z}[U_k^{\text{ext}}] = \int \mathcal{D}U e^{-S_W}, \quad (1.1)$$

where S_W is the standard Wilson action. The functional integration is extended over links on a lattice with the hypertorus geometry and satisfying the constraints

$$U_k(x)|_{x_4=0} = U_k^{\text{ext}}(\vec{x}) \quad k = 1, 2, 3. \quad (1.2)$$

In Eqs. (1.1) and (1.2) $U_\mu^{\text{ext}}(\vec{x})$ is the lattice version of the external continuum gauge field $\vec{A}^{\text{ext}}(\vec{x}) = \vec{A}_a^{\text{ext}}(\vec{x})\lambda_a/2$:

$$U_\mu^{\text{ext}} = \text{P exp} \left\{ ig \int_0^1 dt A_{a,\mu}^{\text{ext}}(x + t\hat{\mu}) \frac{\lambda_a}{2} \right\}, \quad (1.3)$$

where P is the path-ordering operator and g the gauge coupling constant.

The lattice effective action for the background field $\vec{A}^{\text{ext}}(\vec{x})$ is defined by

$$\Gamma[\vec{A}^{\text{ext}}] = -\frac{1}{L_4} \ln \left\{ \frac{\mathcal{Z}[\vec{A}^{\text{ext}}]}{\mathcal{Z}(0)} \right\}, \quad (1.4)$$

where L_4 is the extension in Euclidean time and $\mathcal{Z}(0)$ is the lattice Schrödinger functional, Eq. (1.1), without the external background field ($U_\mu^{\text{ext}} = \mathbf{1}$). It can be shown [31–33] that in the continuum limit $\Gamma[\vec{A}^{\text{ext}}]$ is the vacuum energy in presence of the background field $\vec{A}^{\text{ext}}(\vec{x})$.

To detect the monopole and vortex condensation the relevant quantity turns out to be the following disorder parameter

$$\mu = e^{-E_{\text{bckg}}L_4} = \frac{\mathcal{Z}[\text{bckg}]}{\mathcal{Z}[0]}, \quad (1.5)$$

where $\mathcal{Z}[\text{bckg}]$ is the lattice Schrödinger functional with monopole or vortex background field. According to the physical interpretation of the effective action Eq. (1.4) E_{bckg} is the energy to create a monopole or a vortex in the quantum vacuum.

In the finite temperature case the relevant disorder parameter turns out to be the monopole or vortex free energy [7, 8, 30]. The finite temperature disorder parameter is defined by means of the thermal partition function in presence of the given static background field:

$$\mathcal{Z}_T[\vec{A}^{\text{ext}}] = \int_{U_k(\beta_T, \vec{x})=U_k(0, \vec{x})=U_k^{\text{ext}}(\vec{x})} \mathcal{D}U e^{-S_W}. \quad (1.6)$$

In Eq. (1.6) the integrations are over the dynamical unconstrained links with periodic boundary conditions in the time direction on a lattice with $L_4 = \beta_T$, β_T being the inverse of the physical temperature T_{phys} . As concern the boundary conditions at the spatial boundaries, we keep the fixed boundary conditions $U_k(\vec{x}, x_4) = U_k^{\text{ext}}(\vec{x})$ used in the Schrödinger functional Eq.(1.1). Thus we see that, if we send the physical temperature to zero, then the thermal functional Eq. (1.6) reduces to the zero-temperature Schrödinger functional Eq. (1.1). At finite temperature our gauge-invariant disorder parameter is given by:

$$\mu = e^{-F_{\text{bckg}}/T_{\text{phys}}} = \frac{\mathcal{Z}_T[\text{bckg}]}{\mathcal{Z}_T[0]}, \quad (1.7)$$

where $\mathcal{Z}_T[0]$ is the thermal partition function without background field. From Eq. (1.7) it is now clear that F_{bckg} is the free energy to create a monopole or a vortex. If there is condensation, then $F_{\text{bckg}} = 0$ and $\mu = 1$.

The plane of the paper is as follows. In Section II we study the condensation of vortices and monopoles in the zero temperature lattice U(1) pure gauge theory. In Section III we compare the Abelian monopole and vortex condensation for finite temperature SU(2) lattice gauge theory. Section IV is devoted to the case of SU(3) gauge theory at finite temperature, where, according to the choice of the Abelian subgroup, two different kinds of Abelian monopoles and vortices can be defined. Finally, our conclusions are drawn in Section V.

II. U(1)

In this Section we study the monopole and vortex condensation in the lattice pure gauge U(1) theory at zero physical temperature. We are interested in the lattice effective action Eq. (1.4) with a Dirac magnetic monopole or a magnetic vortex background field.

Let us now discuss firstly the case of the Dirac magnetic monopole background field. In the continuum the magnetic monopole field with the Dirac string in the direction \vec{n} is

$$e\vec{b}(\vec{r}) = \frac{n_{\text{mon}}}{2} \frac{\vec{r} \times \vec{n}}{r(r - \vec{r} \cdot \vec{n})}. \quad (2.1)$$

where, according to the Dirac quantization condition, n_{mon} is an integer and e is the electric charge (magnetic charge = $n_{\text{mon}}/2e$). We consider the gauge-invariant background field action Eq. (1.4) where the external background field is given by the lattice version of the Dirac magnetic monopole field. By choosing $\vec{n} = x_3$ we get:

$$\begin{aligned} U_{1,2}^{\text{ext}}(\vec{x}) &= \cos[\theta_{1,2}^{\text{mon}}(\vec{x})] + i \sin[\theta_{1,2}^{\text{mon}}(\vec{x})], \\ U_3^{\text{ext}}(\vec{x}) &= \mathbf{1}, \end{aligned} \quad (2.2)$$

with

$$\begin{aligned} \theta_1^{\text{mon}}(\vec{x}) &= -\frac{n_{\text{mon}}}{4} \frac{(x_2 - X_2)}{|\vec{x}_{\text{mon}}|} \frac{1}{|\vec{x}_{\text{mon}}| - (x_3 - X_3)}, \\ \theta_2^{\text{mon}}(\vec{x}) &= +\frac{n_{\text{mon}}}{4} \frac{(x_1 - X_1)}{|\vec{x}_{\text{mon}}|} \frac{1}{|\vec{x}_{\text{mon}}| - (x_3 - X_3)}. \end{aligned} \quad (2.3)$$

In Equation (2.3) (X_1, X_2, X_3) are the monopole coordinates and $\vec{x}_{\text{mon}} = (\vec{x} - \vec{X})$. In the numerical simulations we put the lattice Dirac monopole at the center of the time slice $x_4 = 0$. To avoid the singularity due to the Dirac string we locate the monopole between two neighboring sites. We have checked that the numerical results are not too sensitive to the precise position of the magnetic monopole.

To avoid the problem of dealing with a partition function we consider $E'_{\text{mon}} = \partial E_{\text{mon}} / \partial \beta$. It is easy to see that E'_{mon} is given by the difference between the average plaquette obtained from configurations without and with the monopole field:

$$E'_{\text{mon}} = V [\langle \text{Plaquette} \rangle_{n_{\text{mon}}=0} - \langle \text{Plaquette} \rangle_{n_{\text{mon}} \neq 0}], \quad (2.4)$$

where V is the spatial volume.

We performed lattice simulations on 16^4 , 24^4 and 32^4 lattices. Note that the links belonging to the time slice $x_4 = 0$ and to the spatial boundary are constrained, this means that they are not updated during Monte Carlo simulation. So that the contributions to E'_{mon} due to the constrained links must be subtracted, this corresponds to consider only the ‘‘dynamical links’’ in the computation of E'_{mon} .

Since we are measuring a local quantity such as the plaquette, a low statistics (from 1000 up to 5000 configurations) is required in order to get a good estimate of E'_{mon} . In Fig. 1 we report our numerical results for E'_{mon} versus β for three different lattice sizes. We see that in the strong coupling region $\beta \lesssim 1$ the monopole internal energy derivative is zero, insensitive to the lattice size. This means that, according to Eq. (1.5), the disorder parameter $\mu \simeq 1$. On the other hand, near the critical coupling $\beta_c \simeq 1$, E'_{mon} displays a sharp peak which increases by increasing the lattice volume. In the weak coupling region ($\beta \gg \beta_c$) the plateau in E'_{mon} indicates that the monopole energy tends to the classical monopole action which behaves linearly in β .

In order to obtain μ we perform the numerical integration of E'_{mon} :

$$E_{\text{mon}} = \int_0^\beta E'_{\text{mon}} d\beta' \quad (2.5)$$

In Fig. 2 we display the logarithm of the disorder parameter μ versus β . In the confined phase we see that $\ln \mu = 0$, so that Eq. (1.5) tells us that the energy required to create a monopole is zero and therefore monopoles condense in the confined $U(1)$ vacuum.

Correspondingly the disorder parameter μ is different from zero in the confined phase. Moreover numerical data suggest that $\mu \rightarrow 0$ when $\beta \rightarrow \beta_c$ in the thermodynamic limit. Note that the different curves for μ corresponding to increasing lattice sizes seem to cross, suggesting a first order phase transition. Obviously a quantitative estimate of β_c and critical exponents require a finite size scaling analysis.

Let us now consider the case of U(1) magnetic vortices. The continuum gauge potential for a classical magnetic vortex along the \hat{z} -direction with n units of elementary flux $\phi = \frac{2\pi}{e}$ is given by

$$\begin{aligned} A_1^{\text{ext}} &= -\frac{n}{e} \frac{x_2}{(x_1)^2 + (x_2)^2}, \\ A_2^{\text{ext}} &= \frac{n}{e} \frac{x_1}{(x_1)^2 + (x_2)^2}, \\ A_3^{\text{ext}} &= 0. \end{aligned} \tag{2.6}$$

The corresponding lattice links are:

$$\begin{aligned} U_{1,2}^{\text{ext}}(\vec{x}) &= \cos[\theta_{1,2}^{\text{vort}}(\vec{x})] + i \sin[\theta_{1,2}^{\text{vort}}(\vec{x})], \\ \theta_{1,2}^{\text{vort}} &= \mp \frac{x_{2,1}}{(x_1)^2 + (x_2)^2}, \\ U_3^{\text{ext}}(\vec{x}) &= \mathbf{1}. \end{aligned} \tag{2.7}$$

As in the monopole case we evaluated numerically the β -derivative E'_{vort} of the energy to create a vortex. In Fig. 3 we compare the monopole and vortex energy derivative for a 16^4 lattice. We clearly see that in the strong coupling monopoles do condense, while there is no signal of vortex condensation. Moreover, near the critical coupling the vortex internal energy derivative displays rapid oscillations. This is confirmed by looking at the behavior of the disorder parameter μ . Indeed, from Fig. 4 we see that in the confined phase $\ln \mu \simeq 0$ for monopoles (i.e.: the energy E_{mon} to create a monopole is zero). On the other hand $\ln \mu > 0$ for vortices, so it costs energy to create a vortex and therefore there is no vortex condensation in the U(1) confined phase.

Thus, we may conclude that in the U(1) lattice theory the strong coupling confined phase is intimately related to magnetic monopole condensation.

III. SU(2)

In previous works [7, 8] we studied Abelian magnetic monopole condensation in finite temperature SU(2) lattice gauge theory. For SU(2) the maximal Abelian group is an Abelian U(1) group. In the continuum the Abelian monopole field turns out to be

$$g\vec{b}^a(\vec{x}) = \delta^{a,3} \frac{n_{\text{mon}}}{2} \frac{\vec{x} \times \vec{n}}{|\vec{x}|(|\vec{x}| - \vec{x} \cdot \vec{n})}. \tag{3.1}$$

\vec{n} is the direction of the Dirac string and, according to the Dirac quantization condition, n_{mon} is an integer. The lattice links corresponding to the Abelian monopole field Eq. (3.1) can be readily obtained from Eq. (1.3). By choosing $\vec{n} = x_3$ we have:

$$\begin{aligned} U_{1,2}^{\text{ext}}(\vec{x}) &= \cos[\theta_{1,2}^{\text{mon}}(\vec{x})] + i\sigma_3 \sin[\theta_{1,2}^{\text{mon}}(\vec{x})], \\ U_3^{\text{ext}}(\vec{x}) &= \mathbf{1}, \end{aligned} \tag{3.2}$$

with

$$\begin{aligned}\theta_1^{\text{mon}}(\vec{x}) &= -\frac{n_{\text{mon}}(x_2 - X_2)}{4} \frac{1}{|\vec{x}_{\text{mon}}| |\vec{x}_{\text{mon}}| - (x_3 - X_3)}, \\ \theta_2^{\text{mon}}(\vec{x}) &= +\frac{n_{\text{mon}}(x_1 - X_1)}{4} \frac{1}{|\vec{x}_{\text{mon}}| |\vec{x}_{\text{mon}}| - (x_3 - X_3)},\end{aligned}\tag{3.3}$$

where (X_1, X_2, X_3) are the monopole coordinates, $\vec{x}_{\text{mon}} = (\vec{x} - \vec{X})$ and the σ_a 's are the Pauli matrices.

As discussed in Sect. I, at finite temperature the relevant quantity is the disorder parameter, Eq. (1.7), defined by means of the thermal partition function $\mathcal{Z}_T[\text{mon}]$ in presence of the Abelian monopole background field. It is worthwhile to stress that our definition of the disorder parameter is gauge invariant, so that we do not need to perform the Abelian projection to define the Abelian monopole field. The numerical results in Refs. [7, 8] show that the monopole disorder parameter μ is different from zero in the confined phase and suggest that it tends to zero when approaching the critical coupling in the thermodynamic limit. Thus the SU(2) confining vacuum does display the Abelian monopole condensation in accordance with the dual superconductivity hypothesis.

Now we want to discuss what happens if we consider an Abelian vortex field as the background field. In the case of the SU(2) gauge theory the Abelian vortex field on the lattice is given by

$$\begin{aligned}U_{1,2}^{\text{ext}}(\vec{x}) &= \cos[\theta_{1,2}^{\text{vort}}(\vec{x})] + i\sigma_3 \sin[\theta_{1,2}^{\text{vort}}(\vec{x})], \\ U_3^{\text{ext}}(\vec{x}) &= \mathbf{1}, \\ \theta_{1,2}^{\text{vort}}(\vec{x}) &= \mp \frac{n_{\text{vort}}}{2} \frac{x_{2,1}}{(x_1)^2 + (x_2)^2}\end{aligned}\tag{3.4}$$

The derivative of the free energy required to create a vortex

$$F'_{\text{vort}} = \frac{\partial}{\partial \beta} F_{\text{vort}},\tag{3.5}$$

can be easily evaluated as the difference between the average plaquette without the vortex background field (i.e. $n_{\text{vort}} = 0$ and with the vortex background field ($n_{\text{vort}} \neq 0$)

$$F'_{\text{vort}} = V [\langle P \rangle_{n_{\text{vort}}=0} - \langle P \rangle_{n_{\text{vort}} \neq 0}],\tag{3.6}$$

where V is the spatial volume.

Simulations have been performed by means of the APE100 computer using the over-relaxed heat-bath algorithm to update the gauge configurations. Since we are measuring a local quantity such as the plaquette, a low statistics (from 2000 up to 10000 configurations) is required in order to get a good estimate of the derivative of the free energy.

In Fig. 5 we display the derivative of the monopole free energy versus β for $n_{\text{mon}} = 10$ on lattices with $L_t = 4$ and $L_s = 24$. We see that F'_{mon} vanishes at strong coupling and displays a rather sharp peak near $\beta \simeq 2.23$. We expect that this peak corresponds to the finite temperature deconfinement transition. In Fig. 5 we also display the absolute value of the Polyakov loop in the time direction

$$P = \frac{1}{V_s} \sum_{\vec{x}} \frac{1}{2} \text{Tr} \prod_{x_4=1}^{L_t} U_4(\vec{x}, x_4)\tag{3.7}$$

and, indeed, we see that the peak correspond to the rise of $|P|$.

In the weak coupling region the plateau in F'_{mon} indicates that the monopole free energy tends to the classical monopole action which behaves linearly in β . In Fig. 5 we display also the derivative of the Abelian vortex free energy Eq. (3.6) for a vortex with $n_{\text{vort}} = 10$. It turns out that monopoles and vortices data agree within statistical errors. To appreciate better this last point we plotted in Fig. 6 the logarithm of the disorder parameter Eq. (1.7) for monopoles and vortices respectively. Fig. 6 shows clearly that monopoles and vortices agree quite perfectly. Our results strongly suggest that Abelian vortices play a role in the dynamics of the deconfinement.

IV. SU(3)

For SU(3) gauge theory the maximal Abelian group is $U(1) \times U(1)$, therefore we may introduce two independent types of Abelian monopole or Abelian vortex. Let us consider firstly the Abelian monopole field. The first type of Abelian monopole field is derived considering the λ_3 diagonal generator, we name it T_3 Abelian monopole (following Refs. [7, 8]). On the lattice it is given by

$$U_{1,2}^{\text{ext}}(\vec{x}) = \begin{bmatrix} e^{i\theta_{1,2}^{\text{mon}}(\vec{x})} & 0 & 0 \\ 0 & e^{-i\theta_{1,2}^{\text{mon}}(\vec{x})} & 0 \\ 0 & 0 & 1 \end{bmatrix} \quad (4.1)$$

$$U_3^{\text{ext}}(\vec{x}) = \mathbf{1} ,$$

with $\theta_{1,2}^{\text{mon}}(\vec{x})$ defined in Eq. (3.3).

The second type of independent Abelian monopole can be obtained by considering the diagonal generator λ_8 . In this case we have the T_8 Abelian monopole:

$$U_{1,2}^{\text{ext}}(\vec{x}) = \begin{bmatrix} e^{i\theta_{1,2}^{\text{mon}}(\vec{x})} & 0 & 0 \\ 0 & e^{i\theta_{1,2}^{\text{mon}}(\vec{x})} & 0 \\ 0 & 0 & e^{-2i\theta_{1,2}^{\text{mon}}(\vec{x})} \end{bmatrix} \quad (4.2)$$

$$U_3^{\text{ext}}(\vec{x}) = \mathbf{1} ,$$

with

$$\theta_1^{\text{mon}}(\vec{x}) = \frac{1}{\sqrt{3}} \left[-\frac{n_{\text{mon}}(x_2 - X_2)}{4} \frac{1}{|\vec{x}_{\text{mon}}| - (x_3 - X_3)} \right] , \quad (4.3)$$

$$\theta_2^{\text{mon}}(\vec{x}) = \frac{1}{\sqrt{3}} \left[+\frac{n_{\text{mon}}(x_1 - X_1)}{4} \frac{1}{|\vec{x}_{\text{mon}}| - (x_3 - X_3)} \right] .$$

Analogously, we have the T_8 Abelian vortex:

$$U_{1,2}^{\text{ext}}(\vec{x}) = \begin{bmatrix} e^{i\theta_{1,2}^{\text{vort}}(\vec{x})} & 0 & 0 \\ 0 & e^{i\theta_{1,2}^{\text{vort}}(\vec{x})} & 0 \\ 0 & 0 & e^{-2i\theta_{1,2}^{\text{vort}}(\vec{x})} \end{bmatrix} , \quad (4.4)$$

$$U_3^{\text{ext}}(\vec{x}) = \mathbf{1}$$

$$\theta_{1,2}^{\text{vort}} = \mp \frac{1}{\sqrt{3}} \frac{n_{\text{vort}}}{2} \frac{x_{2,1}}{(x_1)^2 + (x_2)^2} ,$$

and the T_3 Abelian vortex:

$$\begin{aligned}
U_{1,2}^{\text{ext}}(\vec{x}) &= \begin{bmatrix} e^{i\theta_{1,2}^{\text{vort}}(\vec{x})} & 0 & 0 \\ 0 & e^{-i\theta_{1,2}^{\text{vort}}(\vec{x})} & 0 \\ 0 & 0 & 1 \end{bmatrix}, \\
U_3^{\text{ext}}(\vec{x}) &= \mathbf{1} \\
\theta_{1,2}^{\text{vort}} &= \mp \frac{n_{\text{vort}}}{2} \frac{x_{2,1}}{(x_1)^2 + (x_2)^2}.
\end{aligned} \tag{4.5}$$

The other Abelian monopoles and vortices can be generated by considering the linear combinations of the λ_3 and λ_8 generators. In particular we have also considered the following two linear combinations of $\lambda^3/2$ and $\lambda^8/2$

$$T_{3a} = -\frac{1}{2} \frac{\lambda^3}{2} + \frac{\sqrt{3}}{2} \frac{\lambda^8}{2} = \begin{bmatrix} 0 & 0 & 0 \\ 0 & \frac{1}{2} & 0 \\ 0 & 0 & -\frac{1}{2} \end{bmatrix}, \tag{4.6}$$

and

$$T'_3 = \frac{\sqrt{3}}{2} \frac{\lambda^3}{2} + \frac{1}{2} \frac{\lambda^8}{2} = \begin{bmatrix} \frac{1}{\sqrt{3}} & 0 & 0 \\ 0 & -\frac{1}{2\sqrt{3}} & 0 \\ 0 & 0 & -\frac{1}{2\sqrt{3}} \end{bmatrix}. \tag{4.7}$$

The linear combinations given in Eq.(4.6) and in Eq.(4.7) have been also considered in Ref. [4, 5] and in Ref. [34] respectively. For reader convenience, let us summarize the main results of our previous investigation of Abelian monopole condensation [7, 8] in SU(3). In Refs. [7, 8] we found that there is condensation of Abelian monopoles in the non perturbative vacuum; moreover lattice data show that the SU(3) vacuum reacts moderately strongly in the case of the T_8 Abelian monopole.

In the present paper we compare the T_8 Abelian monopoles and vortices. In Fig. 7 the free energy derivative for monopoles and vortices is displayed versus β for a lattice with $L_s = 32$ and $L_t = 4$. We also display the absolute value of the Polyakov loop in the time direction

$$P = \frac{1}{V_s} \sum_{\vec{x}} \frac{1}{3} \text{Tr} \prod_{x_4=1}^{L_t} U_4(\vec{x}, x_4). \tag{4.8}$$

As can be argued from Fig. 7, F'_{vort} behaves like F'_{mon} . Indeed, the free energy derivatives are zero within errors in the strong coupling region and display a sharp peak in correspondence of the rise of the Polyakov loop. In the weak coupling region the free energy derivatives are almost constant. The values of the plateau correspond to the beta derivative of the lattice classical action. Remarkably Fig. 7 shows that in the peak region the T_8 Abelian vortex displays a signal higher than the Abelian monopole. This is better appreciated if we look at the disorder parameter Eq. (1.7) (see Fig. 8).

In the study of Abelian monopole condensation we found that in the pattern of dynamical symmetry breaking due to the Abelian monopole condensation the color direction 8 is slightly preferred with respect to the direction 3 in the color space. It is worthwhile to

see if this result holds also for the Abelian vortex condensation. In Figure 9 we compare the free energy derivative for the T_3 and T_8 Abelian vortices for the lattice with $L_t = 4$ and $L_s = 32$. As expected the T_8 Abelian vortex displays a signal about a factor two higher in the peak region. Finally in Fig. 10 and in Fig. 11 we confront the T_3 , T_{3a} , T_8 and T'_3 Abelian vortices. We find the expected result that T_3 and T_8 agree within statistical errors in the whole range of β with T_{3a} and T'_3 respectively. For the sake of completeness we also report in Fig. 12 the comparison between the T'_3 and T_8 monopoles, showing that also for monopoles they agree within statistical errors.

We may conclude that, even in the most interesting case of the SU(3) gauge theory, our results strongly suggest that Abelian vortices play a role in the dynamics of the confinement.

V. CONCLUSIONS

In this paper we have investigated Abelian monopole and vortex condensation in U(1) at zero temperature and in the finite temperature SU(2) and SU(3) lattice gauge theories. In the case of U(1) pure gauge theory we find that the confining vacuum can be interpreted as a coherent condensate of magnetic monopoles. On the other hand, we do not find evidence of condensation of vortices. This is at variance of the non Abelian SU(2) and SU(3) gauge theories where instead we found evidence of Abelian magnetic monopole and vortex condensation. We feel that this result confirms that in the U(1) strong coupling confining region the dual superconductor mechanism is realized by condensation of Dirac magnetic monopoles.

In the case of non Abelian pure gauge theories at finite temperature, by means of the lattice thermal partition functional, we introduced a disorder parameter which signals the Abelian monopole and vortex condensation in the confined phase. By construction our definition of the disorder parameter is invariant against gauge transformation of the external background field. As a consequence we do not need to perform the Abelian projection. Our numerical results suggest that the disorder parameter μ is different from zero in the confined phase and tends to zero when approaching the critical coupling in the thermodynamic limit for both Abelian monopoles and vortices.

For the SU(2) gauge theory we find that disorder parameters for monopoles and vortices agree quite perfectly, signaling that Abelian vortices play a role in the dynamics of the deconfinement temperature. On the other hand, remarkably, in the case of SU(3) gauge theory it turns out that the Abelian vortex displays a signal higher than the Abelian monopole. Moreover, for the Abelian vortices we find that the non perturbative vacuum reacts moderately strongly to the T_8 vortices with respect to T_3 vortices. This last point is in accordance with our finding in the study of SU(3) Abelian monopole condensation [7, 8].

In conclusion it is worthwhile to observe that our results point to a different mechanism of confinement in the case of U(1) lattice gauge theory with respect to SU(2) and SU(3) gauge theories. Indeed, in the U(1) Abelian case we find that the confining vacuum behaves as a coherent condensate of Dirac magnetic monopoles. On the other hand in SU(2) and SU(3) it seems that there is condensation of Abelian magnetic monopoles and vortices. So that in SU(2) and SU(3) gauge theories one could look at the confining vacuum as a coherent Abelian magnetic condensate. Even more, for the SU(3) theory, it turns out that gauge field configurations leading to Abelian magnetic flux tubes, multiple of the elementary flux, seem to be favourite with respect to Abelian magnetic monopoles.

We stress, finally, that it is not clear to us if there is a relation between our Abelian magnetic vortices and the center vortices. Indeed, recently the Authors of Refs. [35, 36] found evidence of center vortices condensation in SU(2) and SU(3) lattice pure gauge theories. So that it should be interesting to extend our method to the case of center vortices. We hope to report progress in this direction in the near future.

References

- [1] G. 't Hooft, in *High Energy Physics, EPS International Conference, Palermo, 1975*.
- [2] S. Mandelstam, Phys. Rept. **23**, 245 (1976).
- [3] A. D. Giacomo, Acta Phys. Polon. **B25**, 215 (1994).
- [4] A. D. Giacomo, B. Lucini, L. Montesi, and G. Paffuti, Phys. Rev. **D61**, 034503 (2000), hep-lat/9906024.
- [5] A. D. Giacomo, B. Lucini, L. Montesi, and G. Paffuti, Phys. Rev. **D61**, 034504 (2000), hep-lat/9906025.
- [6] J. M. Carmona, M. D'Elia, A. D. Giacomo, B. Lucini, and G. Paffuti, (2001), hep-lat/0103005.
- [7] P. Cea and L. Cosmai, Phys. Rev. **D62**, 094510 (2000), hep-lat/0006007.
- [8] P. Cea and L. Cosmai, Nucl. Phys. Proc. Suppl. **83**, 428 (2000), hep-lat/9909056.
- [9] L. D. Debbio, M. Faber, J. Greensite, and S. Olejnik, Phys. Rev. **D55**, 2298 (1997), hep-lat/9610005.
- [10] L. D. Debbio, M. Faber, J. Giedt, J. Greensite, and S. Olejnik, Phys. Rev. **D58**, 094501 (1998), hep-lat/9801027.
- [11] K. Langfeld, H. Reinhardt, and O. Tennert, Phys. Lett. **B419**, 317 (1998), hep-lat/9710068.
- [12] K. Langfeld, O. Tennert, M. Engelhardt, and H. Reinhardt, Phys. Lett. **B452**, 301 (1999), hep-lat/9805002.
- [13] P. de Forcrand and M. D'Elia, Phys. Rev. Lett. **82**, 4582 (1999), hep-lat/9901020.
- [14] R. Bertle, M. Faber, J. Greensite, and S. Olejnik, Nucl. Phys. Proc. Suppl. **83**, 425 (2000), hep-lat/9909002.
- [15] C. Alexandrou, M. D'Elia, and P. de Forcrand, Nucl. Phys. Proc. Suppl. **83**, 437 (2000), hep-lat/9907028.
- [16] J. Ambjorn, J. Giedt, and J. Greensite, Nucl. Phys. Proc. Suppl. **83**, 467 (2000), hep-lat/9908017.
- [17] A. Montero, Nucl. Phys. Proc. Suppl. **83**, 518 (2000), hep-lat/9907024.

- [18] O. Jahn, F. Lenz, J. W. Negele, and M. Thies, Nucl. Phys. Proc. Suppl. **83**, 524 (2000), hep-lat/9909062.
- [19] H. Reinhardt, M. Engelhardt, K. Langfeld, M. Quandt, and A. Schafke, Nucl. Phys. Proc. Suppl. **83**, 536 (2000), hep-lat/9908027.
- [20] J. D. Stack and W. Tucker, Nucl. Phys. Proc. Suppl. **83**, 539 (2000).
- [21] P. W. Stephenson, Nucl. Phys. Proc. Suppl. **83**, 544 (2000), hep-lat/9909022.
- [22] B. L. G. Bakker, A. I. Veselov, and M. A. Zubkov, Nucl. Phys. Proc. Suppl. **83**, 565 (2000).
- [23] G. 't Hooft, Nucl. Phys. **B138**, 1 (1978).
- [24] J. M. Cornwall, Nucl. Phys. **B157**, 392 (1979).
- [25] J. M. Cornwall, Phys. Rev. **D57**, 7589 (1998), hep-th/9712248.
- [26] G. Mack and V. B. Petkova, Ann. Phys. **123**, 442 (1979).
- [27] G. Mack and V. B. Petkova, Ann. Phys. **125**, 117 (1980).
- [28] E. Tomboulis, Phys. Rev. **D23**, 2371 (1981).
- [29] E. T. Tomboulis, Phys. Lett. **B303**, 103 (1993).
- [30] P. Cea and L. Cosmai, Nucl. Phys. Proc. Suppl. **94**, 486 (2001), hep-lat/0010034.
- [31] P. Cea, L. Cosmai, and A. D. Polosa, Phys. Lett. **B392**, 177 (1997), hep-lat/9601010.
- [32] P. Cea and L. Cosmai, Nucl. Phys. Proc. Suppl. **53**, 574 (1997), hep-lat/9607015.
- [33] P. Cea and L. Cosmai, Phys. Rev. **D60**, 094506 (1999), hep-lat/9903005.
- [34] P. de Forcrand and M. Pepe, Nucl. Phys. **B598**, 557 (2001), hep-lat/0008016.
- [35] L. D. Debbio, A. D. Giacomo, and B. Lucini, Nucl. Phys. Proc. Suppl. **94**, 502 (2001), hep-lat/0010044.
- [36] L. D. Debbio, A. D. Giacomo, and B. Lucini, Nucl. Phys. **B594**, 287 (2001), hep-lat/0006028.

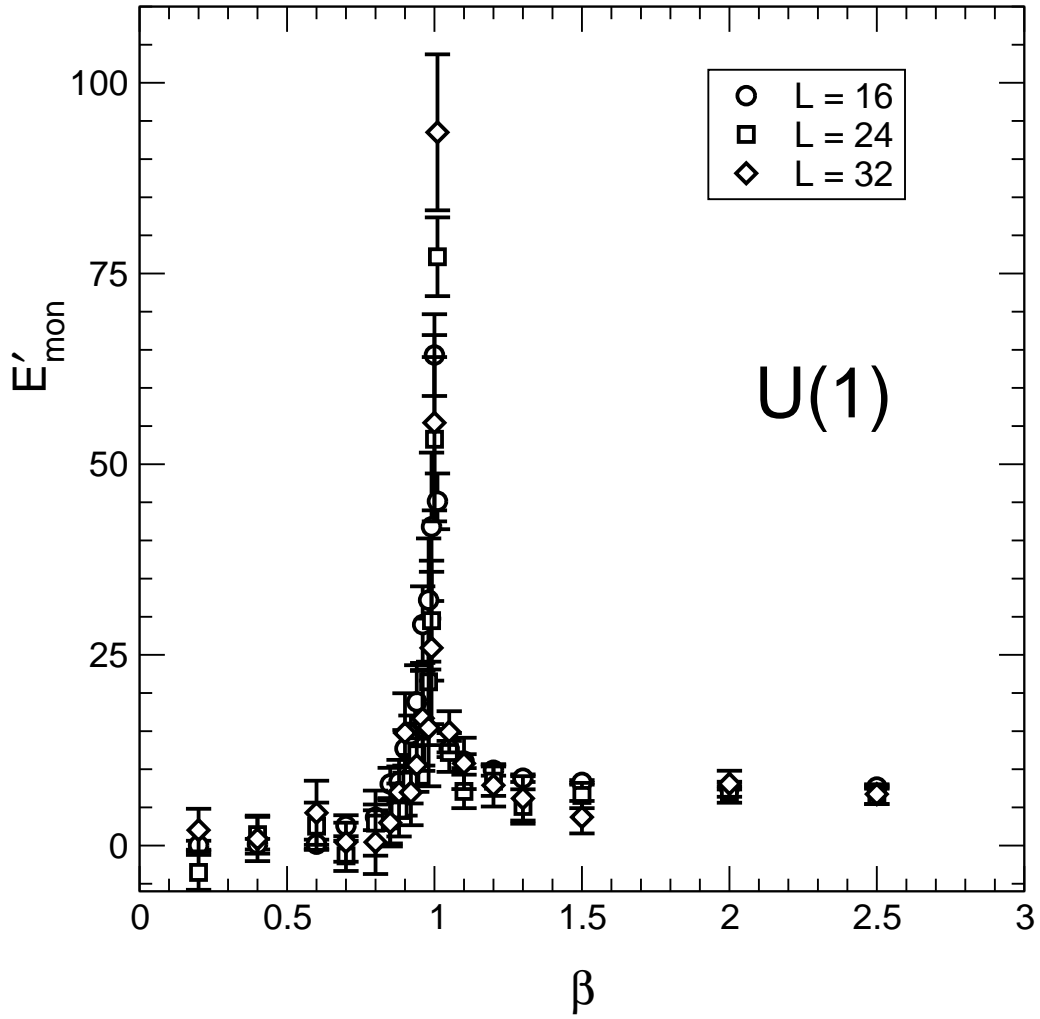


Figure 1: The derivative of the energy to create a monopole, Eq. (2.4), versus β for U(1) lattice gauge theory on a L^4 lattice (circles refer to $L = 16$, squares to $L = 24$, and diamonds to $L = 32$).

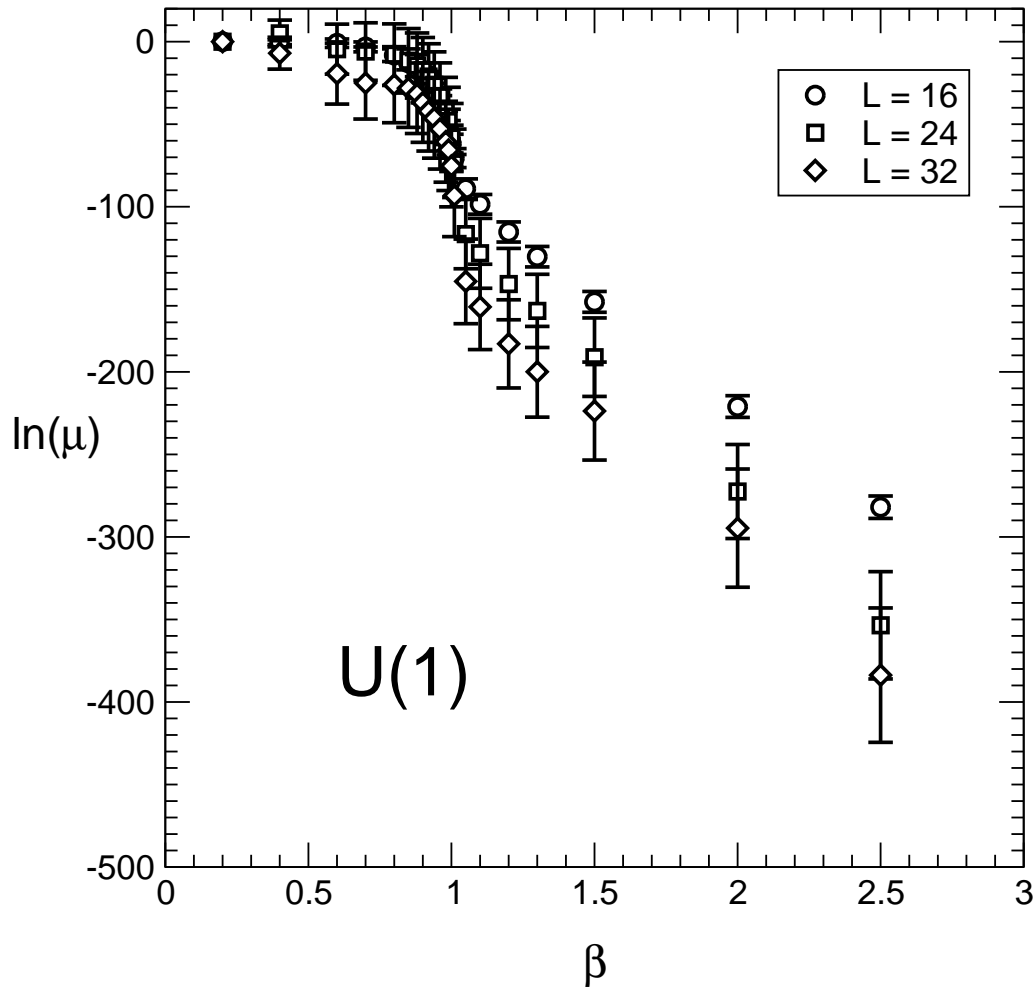


Figure 2: The logarithm of the disorder parameter, Eq. (1.5), versus β for $U(1)$ lattice gauge theory on a L^4 lattice. Symbols as in Fig. 1.

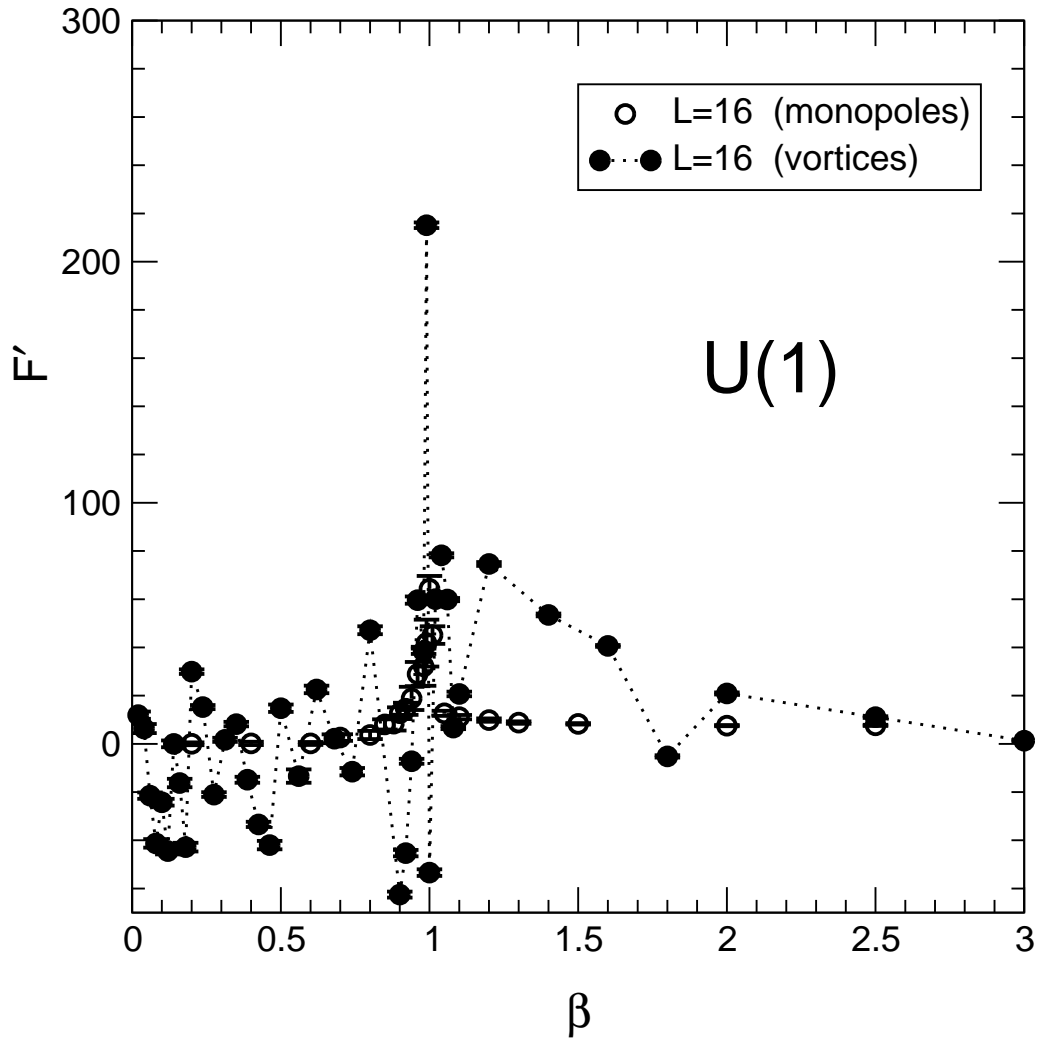


Figure 3: The derivative of the energy to create a monopole or a vortex versus β for U(1) lattice gauge theory on a 16^4 lattice. Open circles refer to a monopole background field and full circles to a vortex background field.

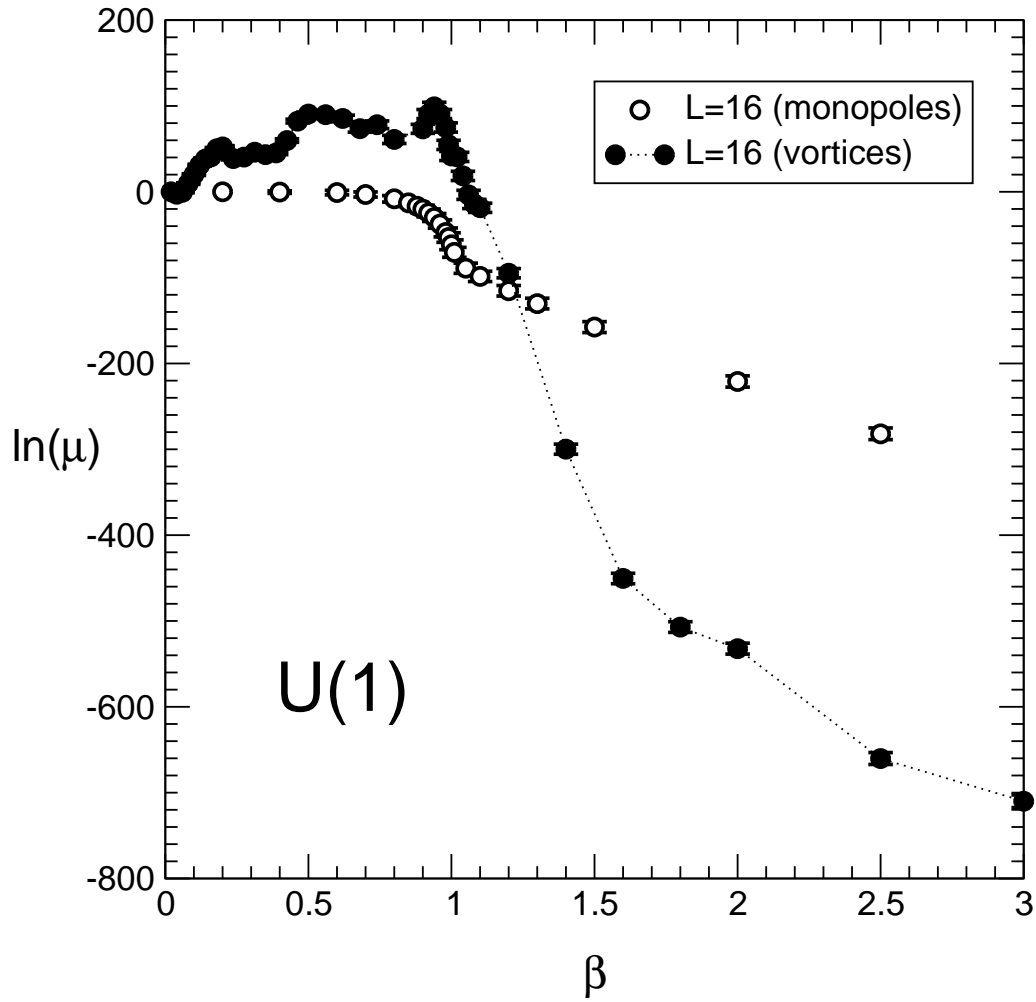


Figure 4: The logarithm of the disorder parameter, Eq. (1.5), versus β for monopoles (open circles) and vortices (full circles) for $U(1)$ on a 16^4 lattice.

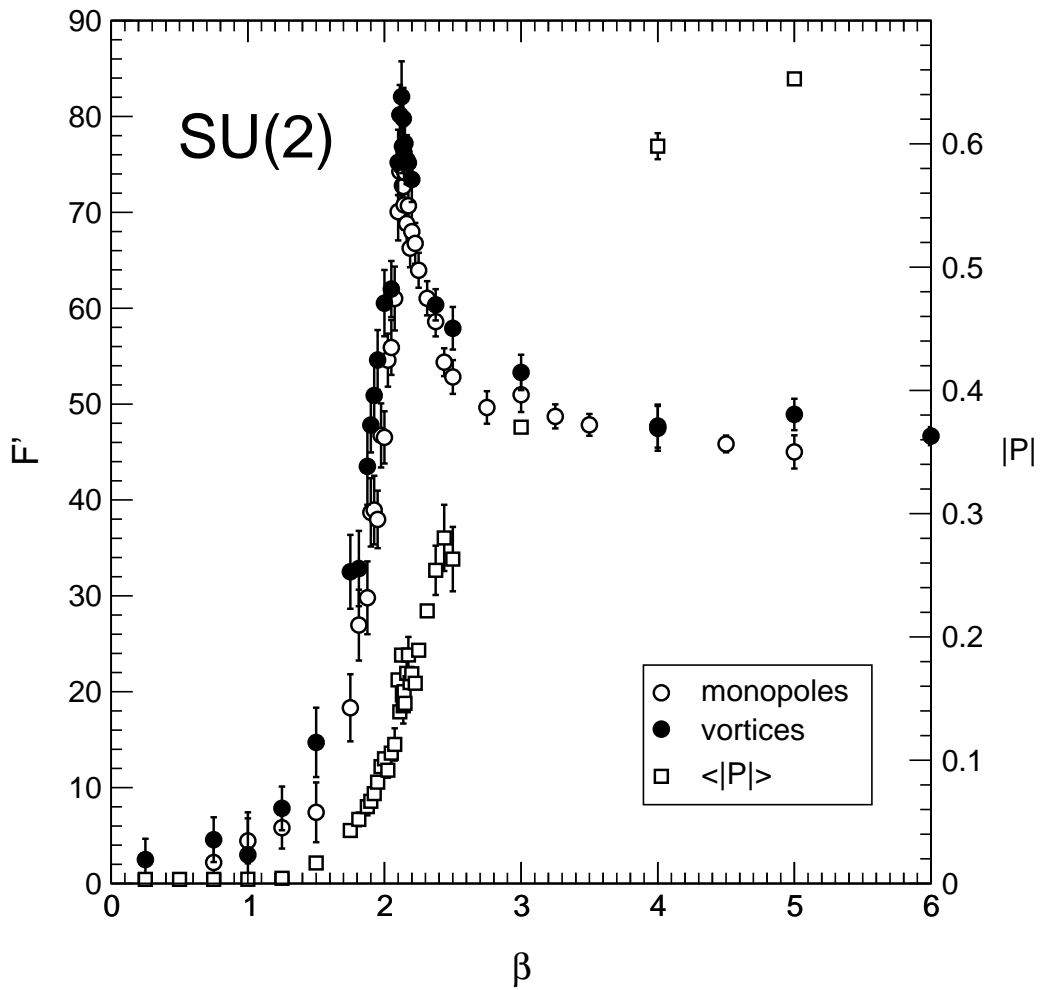


Figure 5: The derivative of the free energy, Eq. (3.5), versus β for monopoles (open circles) and vortices (full circles) for SU(2) on a $24^3 \times 4$ lattice. The absolute value of the Polyakov loop, Eq. (3.7), is also displayed (open squares).

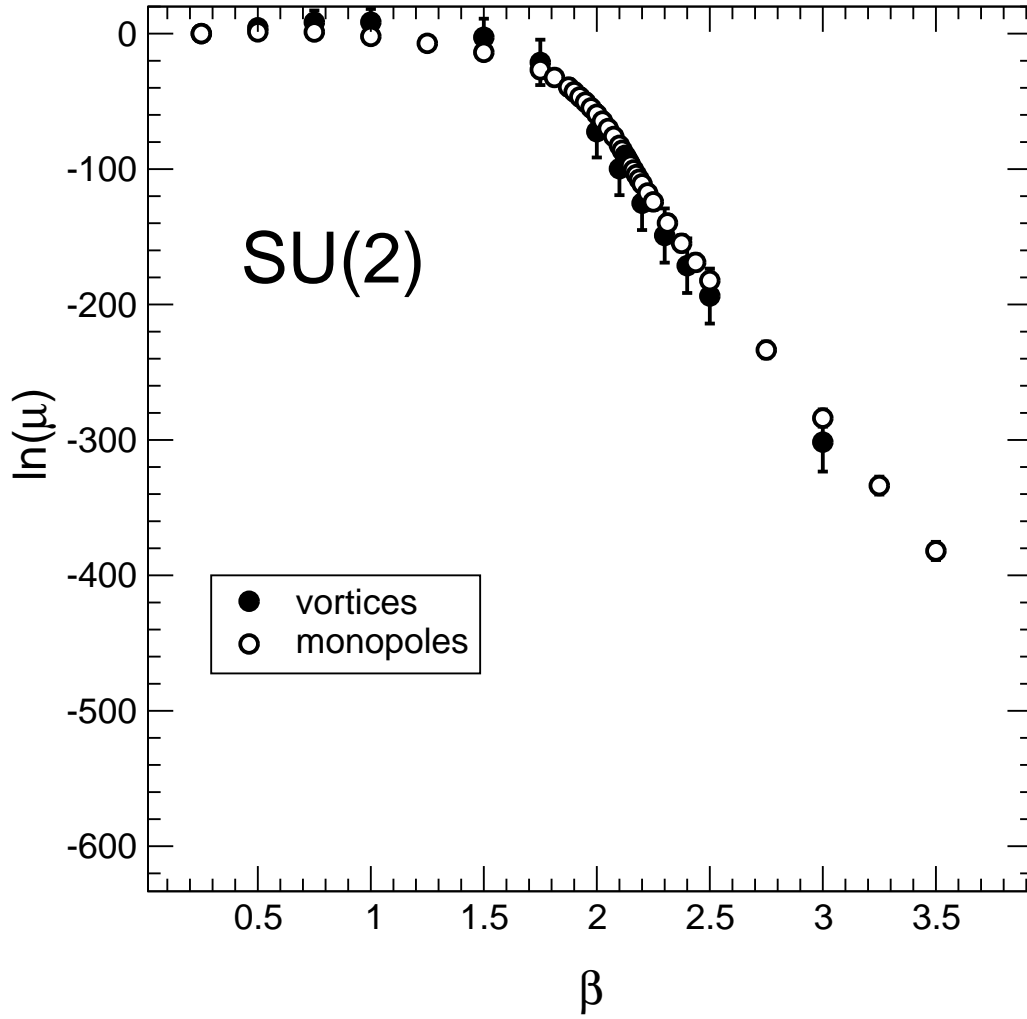


Figure 6: The logarithm of the disorder parameter, Eq. (1.7), versus β for vortices (full circles) and monopoles (open circles). Data refer to SU(2) gauge theory on a $24^3 \times 4$ lattice.

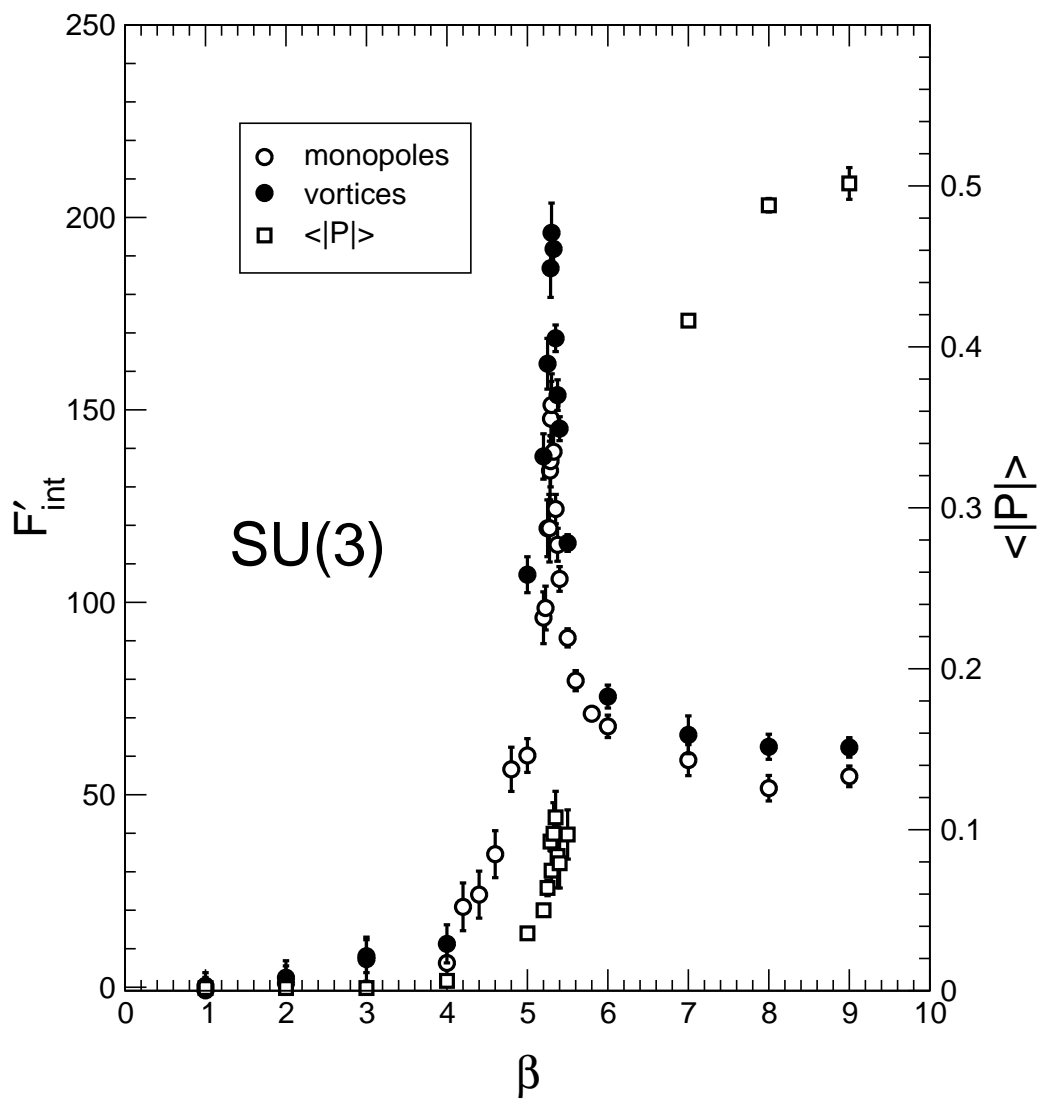


Figure 7: The derivative of the free energy versus β for monopoles (open circles) and vortices (full circles). The absolute value of the Polyakov loop, Eq. (4.8), is also displayed (open squares). Data refer to SU(3) gauge theory on a $32^3 \times 4$ lattice.

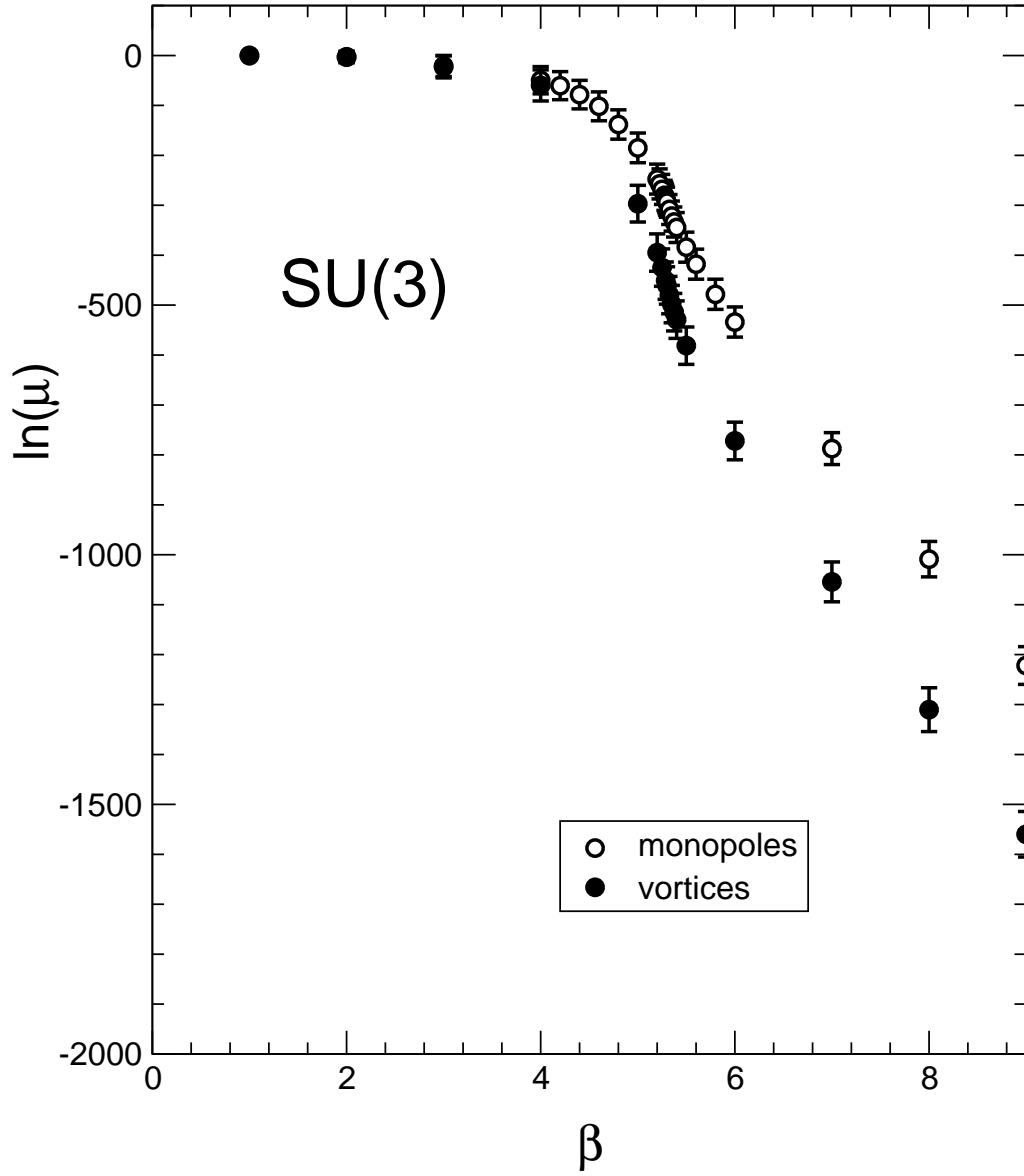


Figure 8: The logarithm of the disorder parameter, Eq. (1.7), versus β for T_8 monopoles (open circles) and T_8 vortices (full circles). Data refer to SU(3) gauge theory on a $32^3 \times 4$ lattice.

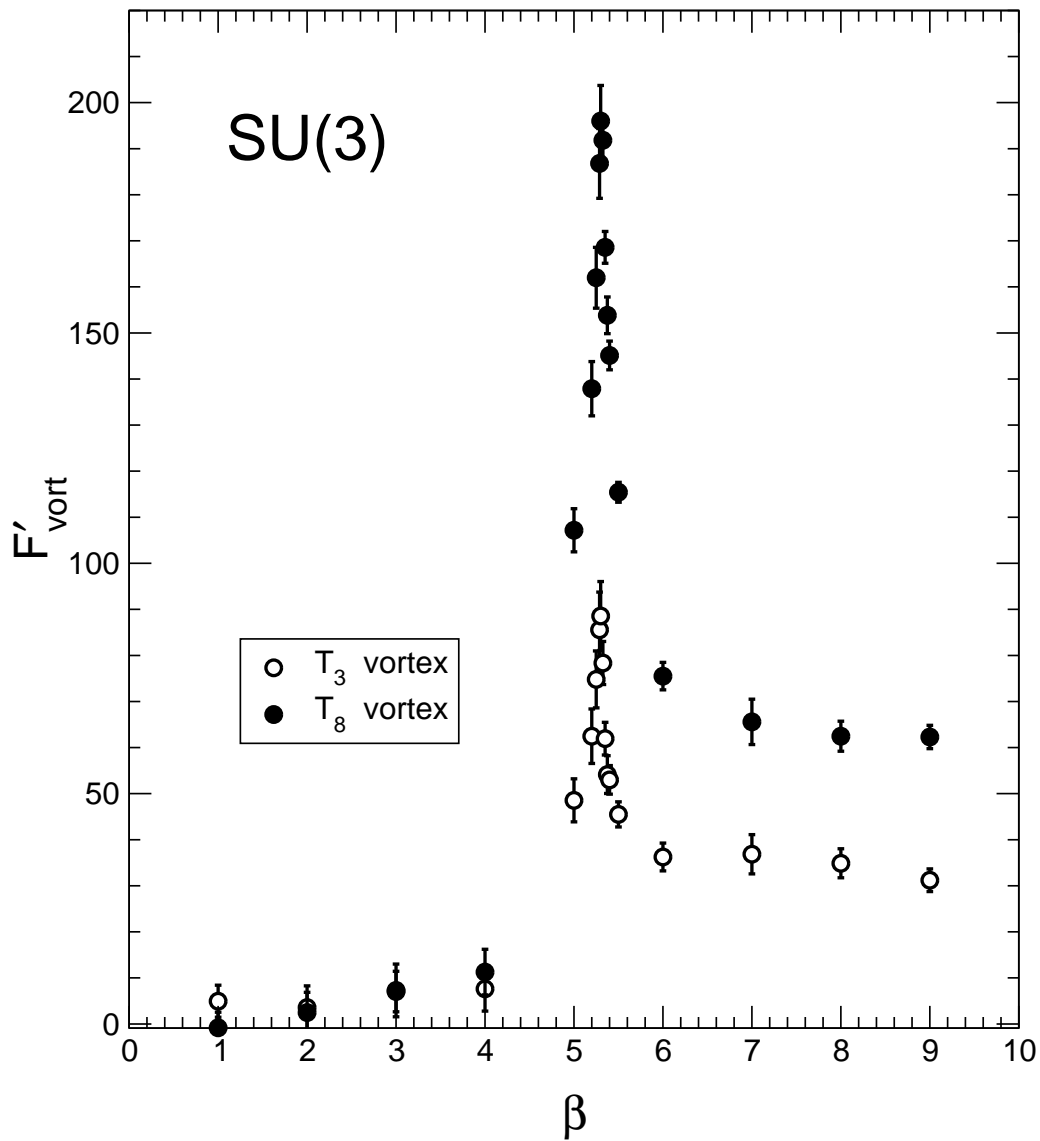


Figure 9: The free energy derivative for T_3 vortices (open circles) and T_8 vortices (full circles) versus β . Data refer to SU(3) gauge theory on a $32^3 \times 4$ lattice.

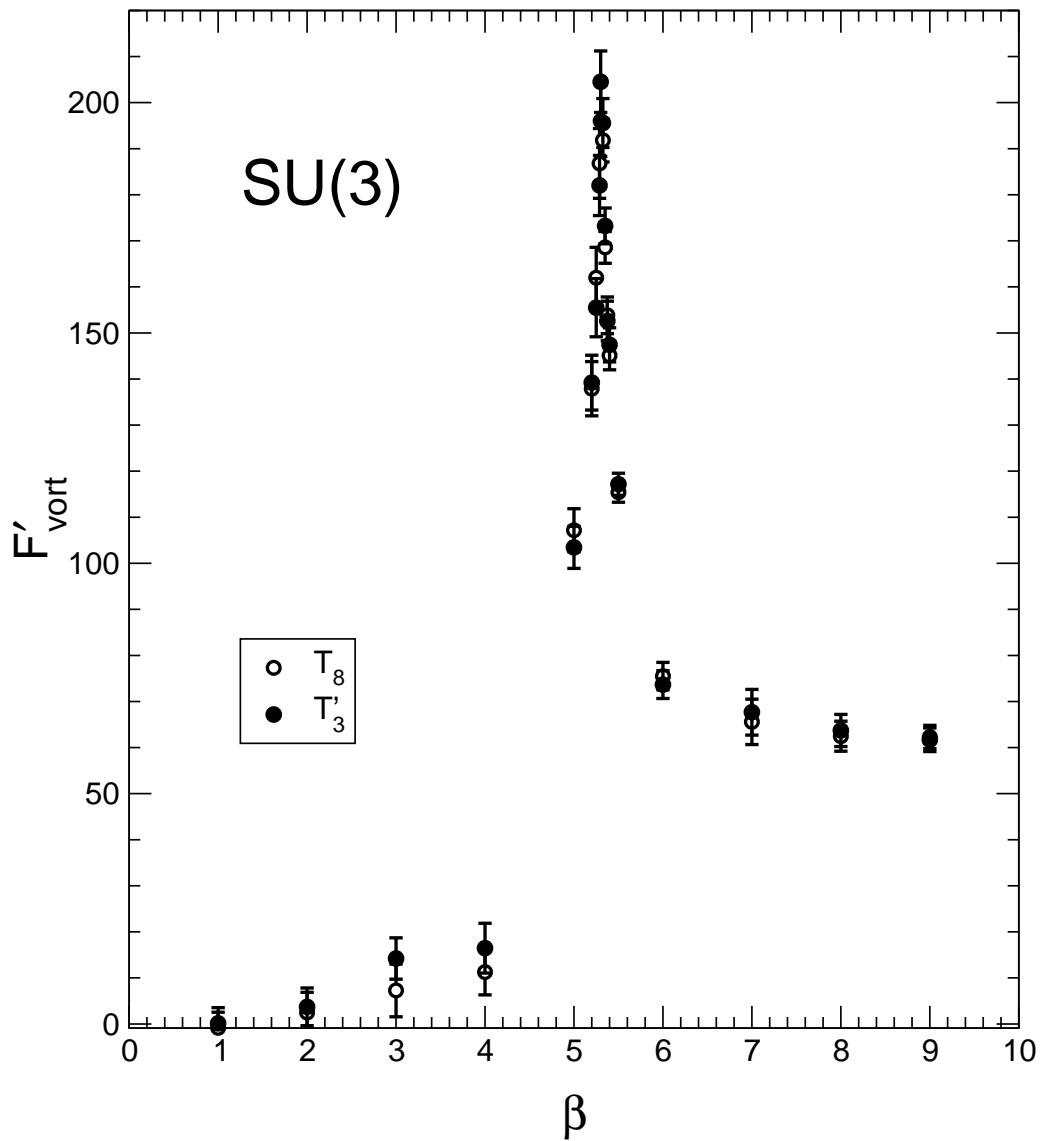


Figure 10: The free energy derivative for T_8 vortices (open circles) and T'_3 vortices (full circles) versus β . Data refer to SU(3) gauge theory on a $32^3 \times 4$ lattice.

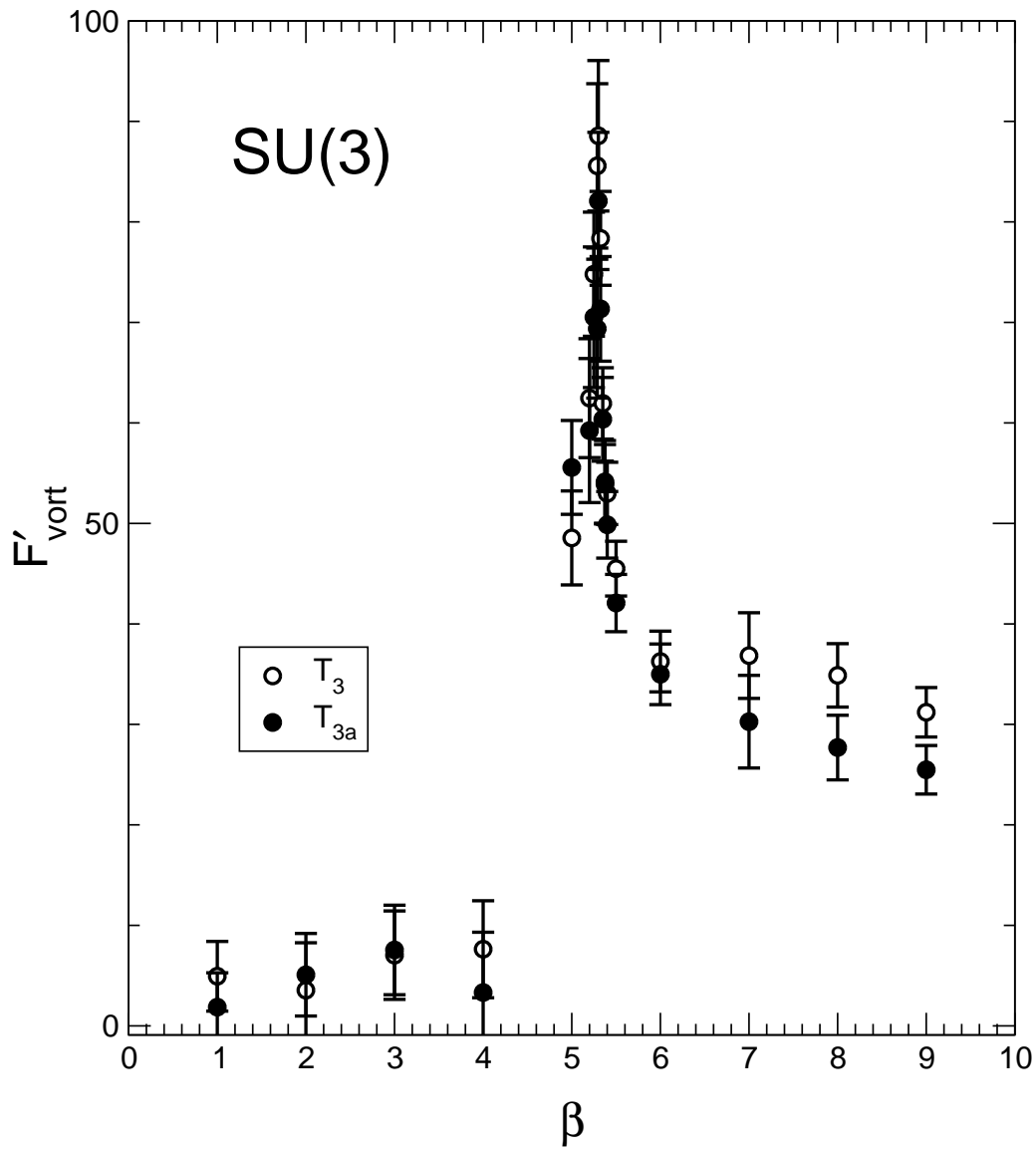


Figure 11: The free energy derivative for T_3 vortices (open circles) and T_{3a} vortices (full circles) versus β . Data refer to SU(3) gauge theory on a $32^3 \times 4$ lattice.

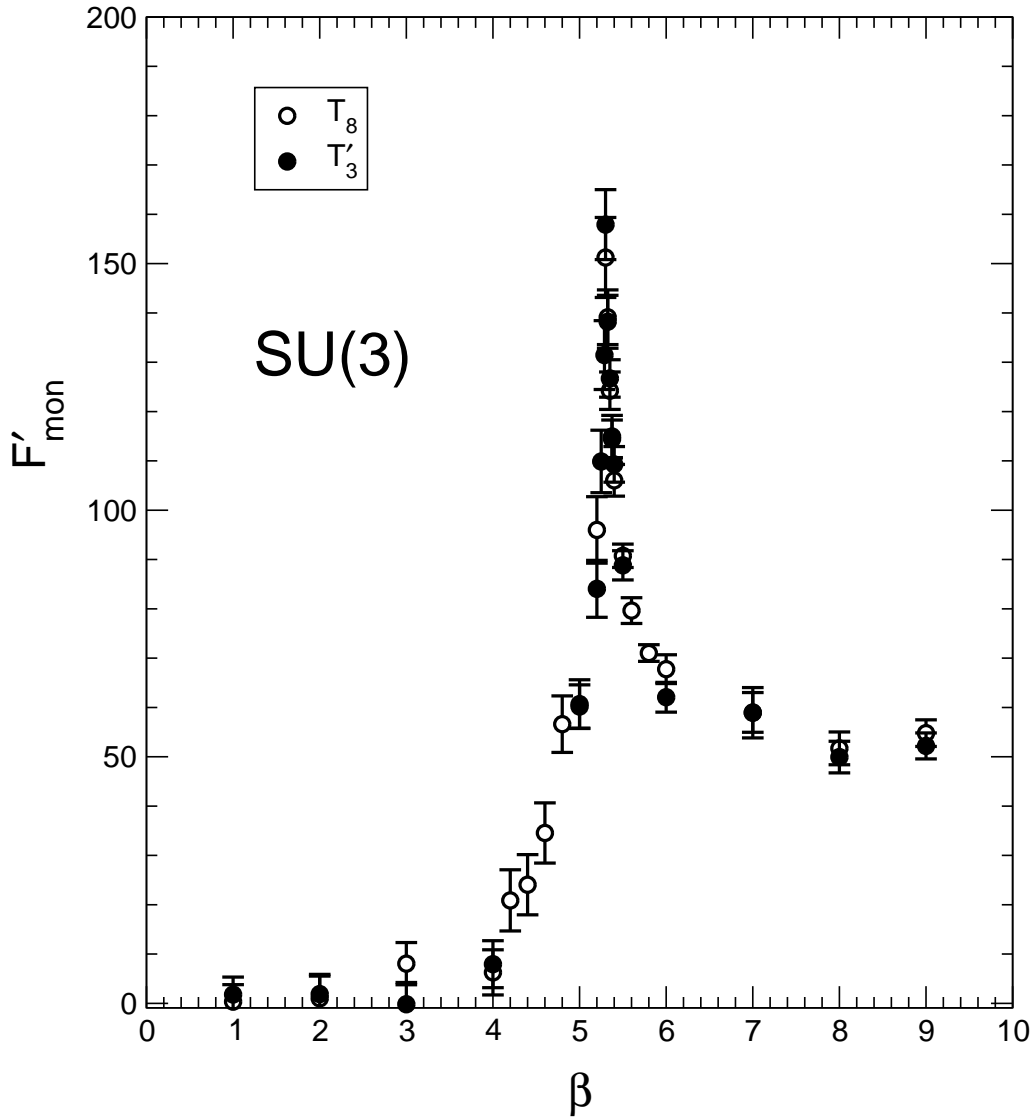


Figure 12: The free energy derivative for T_8 monopoles (open circles) and T'_3 monopoles (full circles) versus β . Data refer to SU(3) gauge theory on a $32^3 \times 4$ lattice.